

Micromachined Fabry–Perot resonator combining submillimeter cavity length and high quality factor

M. Malak,^{1,a)} N. Pavy,¹ F. Marty,¹ Y.-A. Peter,² A. Q. Liu,³ and T. Bourouina^{1,b)}

¹Laboratoire ESYCOM, ESIEE-Paris, Université Paris-Est, Noisy-le-Grand, F-93162 France

²Ecole Polytechnique de Montréal, Montréal, Québec, H3C 3A7 Canada

³School of Electrical and Electronic Engineering, Nanyang Technological University, 639798 Singapore

(Received 5 January 2011; accepted 6 May 2011; published online 26 May 2011)

We demonstrate experimentally optical quality factor of nearly 9000 in a micromachined Fabry–Pérot resonator based on free space propagation of light and direct coupling to optical fibers. This result is obtained on long cavity resonators ($L > 250 \mu\text{m}$), a usually difficult case in terms of power loss, but very useful configuration for experiments requiring either long optical path or enough space for manipulation. The resonator architecture includes two multilayered silicon-air Bragg mirrors of cylindrical shape, combined with a fiber rod lens. The specific stability criteria are derived for the proposed resonator architecture. Dimensions of the fabricated devices are chosen accordingly. © 2011 American Institute of Physics. [doi:10.1063/1.3595277]

Submillimeter Fabry–Pérot (FP) resonators with free space propagation, became important building blocks for many applications, namely, in tunable laser sources,¹ refractometry,² wavelength selection in optical communication,³ as well as chemical sensing.⁴ Tunability of the cavity length is also being routinely integrated thanks to the recent advances in microelectromechanical systems technologies. In most of those applications, the system performance is proven to be mainly dependent on the quality factor (Q -factor) and the finesse of the FP response.

With particular interest to long ($>100 \mu\text{m}$) air cavity microresonators, our objective is to maintain significantly large values for the Q -factor, which is the main point addressed hereafter. In addition to the required high optical quality of the cavity mirrors, their thermomechanical behavior is also of primary importance in fundamental studies involving optomechanical coupling.^{5,6} Therefore, *coating-free* single-crystalline silicon mirrors became very attractive⁷ in this area. Micromachined silicon Bragg mirrors fulfill both requirements of high reflectivity and monolithic nature. Such Bragg mirrors consist of a stack of silicon-air wall pairs, obtained by deep reactive ion etching (DRIE) of trenches on a silicon substrate. At least five groups already reported on FP resonator based on such silicon-air Bragg mirrors fabricated either by DRIE (Refs. 2, 3, 8, and 9) or by etching using aqueous potassium hydroxide.¹⁰ In all these cases, Bragg mirrors were *planar* and the cavity length was in the order of tens of micrometers only, probably for the purpose of reducing the dominant loss mechanism, which relates to expansion of the Gaussian beam inside the cavity after several round trips. Nevertheless, these planar FP cavities are considered as “unstable resonators”¹¹ with Q -factor mostly limited to a few hundreds, except in Ref. 8, where silicon rib-waveguide was introduced leading to $Q=4200$.

In order to overcome the limited performance of conventional planar FP microresonators and in order to enable increasing the cavity length over the ten micrometer range, we

introduce an FP architecture (schematically depicted in Fig. 1), in which we provided two major design improvements. (i) One of these takes advantage of the *cylindrical Bragg mirrors* that act as high reflectivity and concave mirrors. So, they produce focusing of the light beam along one transverse direction, (in-plane). (ii) The other improvement concerns the fiber rod lens (FRL) that has been introduced inside the cavity gap for the purpose of focusing the light beam in another transverse direction (out-of-plane). This combination provides a complete focusing solution, leading to light confinement inside the cavity.

The fabricated devices share common parameters. Every silicon layer has a width of $3.67 \mu\text{m}$ while the air layer has a width of $3.49 \mu\text{m}$. A long recess opening of $128 \mu\text{m}$ width facilitates the insertion of the FRL, whose width is $125 \mu\text{m}$. On the contrary, the fabricated FP cavities differ from each other, either in their physical cavity length, mirror

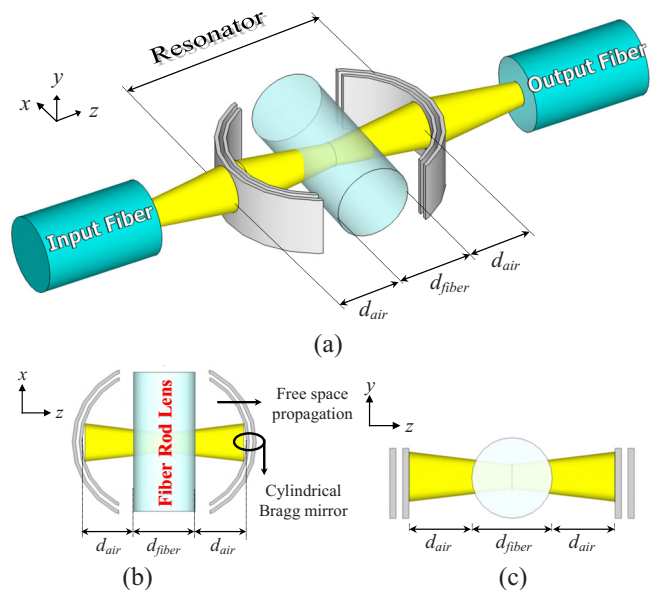


FIG. 1. (Color online) (a) Three-dimensional view of the proposed FP microresonator architecture (b) Cross section view in the XZ plane (c) Cross section view in the YZ plane. The functions of in-plane and out-of-plane focusing are described, respectively.

^{a)}Electronic mail: malakkam@esiee.fr.

^{b)}Author to whom correspondence should be addressed. Electronic mail: t.bourouina@esiee.fr.

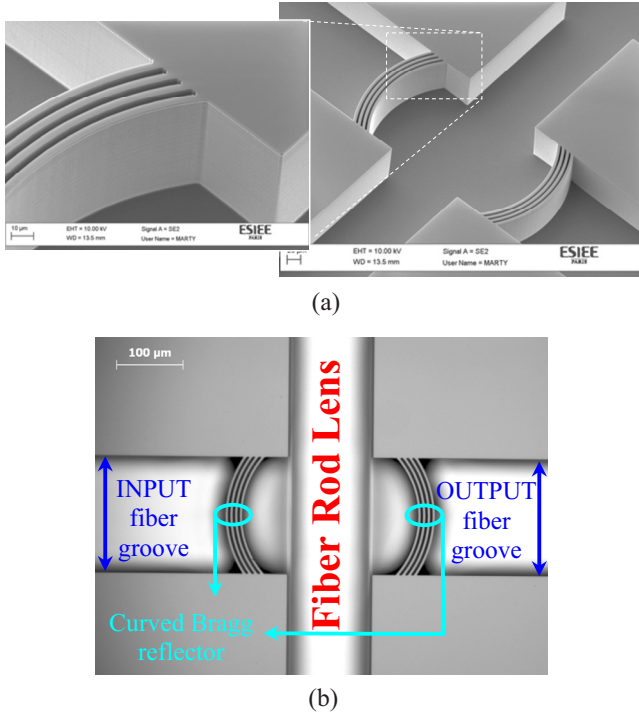


FIG. 2. (Color online) SEM photos of FP cavity architecture (a) Result of silicon micromachining showing the two cylindrical Bragg mirrors (in this case four silicon-air layers each) and the trench for the FRL, (b) with the FRL placed inside the recess.

radius of curvature R or in the number (N) of Bragg layers per mirror. Based on these settings, many combinations were generated, measured and then analyzed. Examples of the fabricated devices are shown in the scanning electron microscope (SEM) photos of Fig. 2.

It is noteworthy that the cavity length and mirror radii of curvature were carefully chosen. Indeed, due to the added FRL inside the air cavity, the well-known stability conditions related to homogeneous spherical mirror cavities¹¹ no longer apply here. In our case, the resonator stability is achieved thanks to two sets of cylindrical surfaces, which are perpendicular to each other. A brief outline of the developed analytical relations, used for optimization and design purposes is presented hereafter.

Each part of the optical resonator was modeled using the ABCD matrix formalism.¹¹ Due to the Gaussian nature of the light beam, it can potentially expand along both x and y directions but it is actually refocused here by two different sets of cylindrical surfaces. Then, we consider that stability conditions must be fulfilled simultaneously in the following two cases, also corresponding to the two transverse cross sections of the device presented in Fig. 1.

- (i) We start by considering the system seen in the XZ cross-section, as schematized in Fig. 1(b), we get the following foremost condition for the range of dimensions leading to stable behavior:

$$0 \leq \frac{2d_{\text{air}} + d_{\text{fiber}}/n_f}{2|R|} \leq 1. \quad (1)$$

- (ii) Then, we analyze the stability of the system seen in the YZ cross section, as schematized in Fig. 1(c). The second stability condition is then found to be as follows:

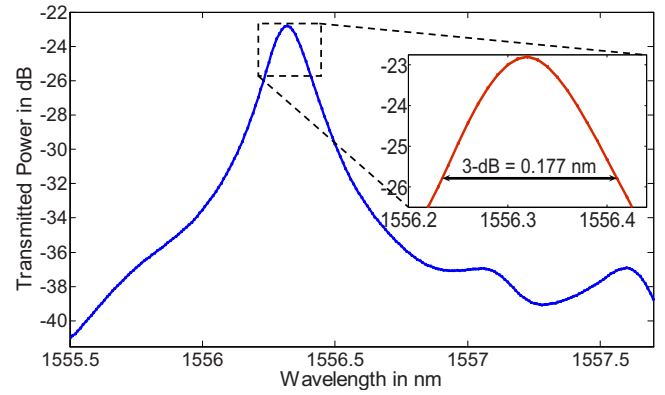


FIG. 3. (Color online) Measured Q -factor of 8818 on a cavity of length $L=265.8 \mu\text{m}$, designed with cylindrical mirrors of radius of curvature $R=140 \mu\text{m}$ with four silicon-air Bragg layers.

$$0 \leq \frac{n_f - 2}{n_f} + 4 \frac{d_{\text{air}}}{d_{\text{fiber}}} \left(\frac{n_f - 1}{n_f} \right) \leq 1, \quad (2)$$

d_{air} and d_{fiber} are the cavity dimensions defined in Fig. 1. R is the radius of curvature of the cylindrical mirrors. n_f is the refractive index of the FRL considered homogeneous over its whole cylindrical volume. By solving Eqs. (1) and (2) for d_{air} , we obtain two different stability ranges related to Gaussian beam expansion along the X and Y directions, also referred previously as YZ and XZ planes, respectively. This means that the cavity might be stable along one direction and unstable along the other. So, whenever we design FRL cavities, we shall look for the values of d_{air} that satisfies both inequalities (1) and (2) for a given mirror radius of curvature R , the FRL diameter d_{fiber} being fixed and equal to $125 \mu\text{m}$.

The fabricated devices were tested using in-plane injection and detection by cleaved fibers. A tunable laser source is used in conjunction with a power-meter for achieving the wavelength sweep and recording the spectral response. The minimum recorded full width at half maximum (FWHM) is 0.1765 nm leading to a Q -factor of 8818. These values are obtained for a cavity having four silicon-air layers per mirror and a physical length $L=265.8 \mu\text{m}$ ($L=2d_{\text{air}} + d_{\text{fiber}}$). Figure 3 shows the measured spectral response of this device. It is noteworthy, in our case, that the physical length is different from the optical length due to the presence of the FRL whose refractive index is $n_f=1.47$. Thus, the optical length is equal in this case to $324.6 \mu\text{m}$.

A simple test has been done to highlight the importance of the FRL on the cavity performance. In this test, a design based on two silicon-air layers per mirror has been measured with and then without insertion of the FRL. Though the reflectance of the two silicon-air layers is not very high, this device has been chosen for this specific illustration because it obeys the stability conditions in both cases (with and without the FRL). Measurements show that the Q -factor improves by a factor of $3.68 \times$ for resonance wavelength around 1615 nm . The obtained results are shown in Fig. 4. One can also notice from this figure, as well as in Fig. 3, additional resonances of smaller amplitude, which are typical of the transverse modes (Hermite-Gaussian), which can appear in optical resonators with curved mirrors.¹¹

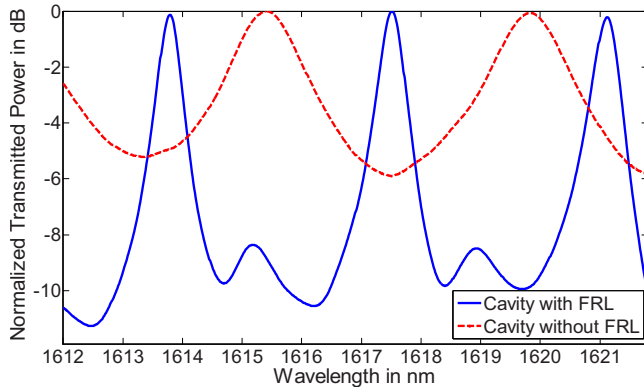


FIG. 4. (Color online) Comparison of measured responses with and without the FRL, illustrating the (3.68x) improvement in the Q -factor. (Here the mirrors consist of two silicon-air layers.)

Other devices with different number (N) of Bragg layers were tested to study the impact of the mirror reflectance \mathfrak{R} on the Q -factor. Figure 5 illustrates the dependence of the Q -factor on to the number of Bragg layers (and hence on the theoretically estimated mirror reflectance \mathfrak{R}) for two sets of cavities having different dimensions. As expected, we find that the Q -factor increases as the number of layers increases till $N=4$. Increasing N beyond 4 creates decrease in the overall Q -factor. Regarding the dependence of the Q -factor with respect to cavity length L , the conclusion is less straightforward, as we roughly have the following trend:

$$Q = \frac{2\pi n_{\text{eff}} L}{\lambda_0} \left[\frac{\sqrt{\mathfrak{R} e^{-2\alpha L}}}{1 - \mathfrak{R} e^{-2\alpha L}} \right], \quad (3)$$

where n_{eff} is the cavity effective refractive index, λ_0 the free space wavelength, and $e^{-2\alpha L}$ an attenuation factor due to the round-trip loss inside the cavity, due mainly to Gaussian beam expansion. Equation (3) suggests that both the value of L and α (effectiveness of beam focusing) will affect the Q -factor. In our case, it appears from Fig. 5 that cavities with the smallest radius R and length L exhibit the highest Q -factor.

In conclusion, we demonstrated a significant improvement to the Q -factor with respect to the conventional planar FP microcavities operated in free-space with direct coupling to optical fibers. This improvement was obtained by introducing a resonator architecture combining curved Bragg mirrors together with FRL, for the purpose of keeping the Gaussian beam focused after the multiple reflections inside the cavity while keeping in the same time the benefit of high reflectance provided by using Bragg mirrors. The proper choice of the resonators dimensions was done according to

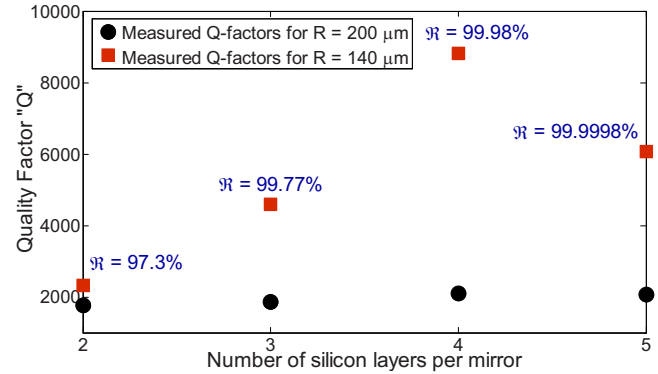


FIG. 5. (Color online) Measured Q -factor vs the number N of Bragg layers per curved mirrors. The corresponding expected theoretical reflectances are indicated along with the experimental data points. Results on two sets of cavities are presented: One set has an optical length $L=265.8 \mu\text{m}$ and radius of curvature $R=140 \mu\text{m}$. The other set has $L=385.6 \mu\text{m}$ and $R=200 \mu\text{m}$.

the outlined analytical model for stability conditions. Measurement results show that a Q -factor of 8818 was obtained for a cavity with four silicon-air layers having a physical length of $265.8 \mu\text{m}$, which represents a breakthrough for submillimeter cavity gap lengths. Furthermore the monolithic nature of the Bragg reflectors and the corresponding single crystalline silicon “ribs” offer another interesting prospect; the cavity can be seen as a natural optomechanically coupled system, in which the movable mass and flexural resonance frequency are in the order of 100 pg and 1 MHz, respectively. The experimental observation of thermal motion of the reflectors through the cavity optical transmission is now among our next targets.

- ¹H. Cai, B. Liu, X. M. Zhang, A. Q. Liu, J. Tamil, T. Bourouina, and Q. X. Zhang, *Opt. Express* **16**, 16670 (2008).
- ²R. St.-Gelais, J. Masson, and Y.-A. Peter, *Appl. Phys. Lett.* **94**, 243905 (2009).
- ³B. Saadany, M. Malak, M. Kubota, F. Marty, Y. Mita, D. Khalil, and T. Bourouina, *IEEE J. Sel. Top. Quantum Electron.* **12**, 1480 (2006).
- ⁴M. J. Thorpe, D. Balslev-Clausen, M. S. Kirchner, and J. Ye, *Opt. Express* **16**, 2387 (2008).
- ⁵D. Kleckner and D. Bouwmeester, *Nature (London)* **444**, 75 (2006).
- ⁶O. Arcizet, P.-F. Cohadon, T. Briant, M. Pinard, and A. Heidmann, *Nature (London)* **444**, 71 (2006).
- ⁷F. Brückner, D. Friedrich, T. Clausnitzer, M. Britzger, O. Burmeister, K. Danzmann, E.-B. Kley, A. Tünnermann, and R. Schnabel, *Phys. Rev. Lett.* **104**, 163903 (2010).
- ⁸M. W. Pruessner, T. H. Stievater, and W. S. Rabinovich, *Appl. Phys. Lett.* **92**, 081101 (2008).
- ⁹S. Yun and J. Lee, *J. Micromech. Microeng.* **13**, 721 (2003).
- ¹⁰A. Lipson and E. M. Yeatman, *Opt. Lett.* **31**, 395 (2006).
- ¹¹A. Yariv, *Quantum Electronics* (Wiley, New York, 1989).